The Plant Cell, Vol. 2, 1009–1017, October 1990 © 1990 American Society of Plant Physiologists

Nodulin Gene Expression and ENOD2 Localization in Effective, Nitrogen-Fixing and Ineffective, Bacteria-Free Nodules of Alfalfa

Clemens Van de Wiel,[a] Joanna H. Norris,[b] Birgit Bochenek,[c] Rebecca Dickstein,[d,1] Ton Bisseling,[a] and Ann M. Hirsch[c,2]

[a] Department of Molecular Biology, Agricultural University, Wageningen, The Netherlands
[b] Department of Botany, University of Rhode Island, Kingston, Rhode Island 02881
[c] Department of Biology, University of California, Los Angeles, California 90024
[d] Department of Genetics, Harvard Medical School and Department of Molecular Biology, Massachusetts General Hospital, Boston, Massachusetts 02114

Alfalfa plants form bacteria-free nodules in response to a number of agents, including *Rhizobium meliloti exo* mutants, *Agrobacterium tumefaciens* transconjugants carrying cloned *R. meliloti* nodulation genes, and compounds that function as auxin transport inhibitors, *N*-(1-naphthyl)phthalamic acid or 2,3,5-triiodobenzoic acid. These bacteria-free nodules contain transcripts for the nodulins Nms30 and MsENOD2; transcripts for late nodulins like leghemoglobin are not detected. In situ hybridization studies demonstrated that ENOD2 transcripts were localized in parenchyma cells at the base and along the periphery of nitrogen-fixing alfalfa root nodules. The ENOD2 gene was also expressed in a tissue-specific manner in nodules elicited by *N*-(1-naphthyl)phthalamic acid and 2,3,5-triiodobenzoic acid. In bacteria-free nodules induced by *R. meliloti exo* mutants and *A. tumefaciens* transconjugants carrying either one or both *R. meliloti* symbiotic plasmids, ENOD2 transcripts were also detected but were usually localized to parenchyma cells at the base instead of along the periphery of the nodule. On the basis of the pattern of ENOD2 gene expression, we conclude that the developmental pathway of bacteria-free nodules, whether bacterially or chemically induced, is the same as that of nitrogen-fixing nodules, and, furthermore, that the auxin transport inhibitors in their action mimic some factor(s) that trigger nodule development.

INTRODUCTION

Alfalfa root nodule development represents an excellent model system for investigating the question of how differentiated root cortical cells escape their developmental destiny and initiate a new structure, the nodule. Alfalfa root nodule development begins after specific recognition of the host plant and *Rhizobium meliloti*. The inner cortical cells of the root divide anticlinally and initiate a nodule primordium, which is soon invaded by an infection thread that originated in an infected root hair (Dudley et al., 1987). Rhizobia are released from branches of the infection thread into cells of the central part of the nodule primordium. Shortly thereafter, the persistent nodule meristem, consisting of small, densely cytoplasmic, actively dividing cells, is organized at the apical (distal) end of the nodule primordium.

The meristem gives rise to cells that differentiate into the central tissue consisting of infected and uninfected cells, the nodule cortex (formerly called "outer cortex"), and the nodule parenchyma (formerly called "inner cortex") (Van de Wiel et al., 1990). The nodule cortex is bounded at its inner side by the nodule endodermis, whereas the nodule parenchyma is located between the central tissue of infected and uninfected cells and the nodule cortex. Nodule parenchyma tissue consists of highly vacuolated parenchyma cells that are more densely packed, with fewer and smaller intercellular spaces, than the nodule cortex. Nodule parenchyma also develops at the base of the nodule. Thus, the central tissue of the nodule is completely surrounded by nodule parenchyma, except at the distal end where the apical meristem is situated. This arrangement of cells has been related to nodule parenchyma's property of forming a barrier to the penetration of free oxygen toward the central tissue (cf Witty et al., 1986).

As is the case for many legumes, alfalfa nodule development can be arrested at several different stages. However, alfalfa roots are more susceptible than many other legumes to agents that elicit the formation of ineffective, bacteria-free nodules. *R. meliloti* mutants defective in ex-

[1] Current address: Laboratoire de Biologie Moléculaire des Relations Plantes-Microorganismes, CNRS-INRA, Chemin de Borderouge, BP 27, 31326 Castanet-Tolosan Cedex, France.
[2] To whom correspondence should be addressed.

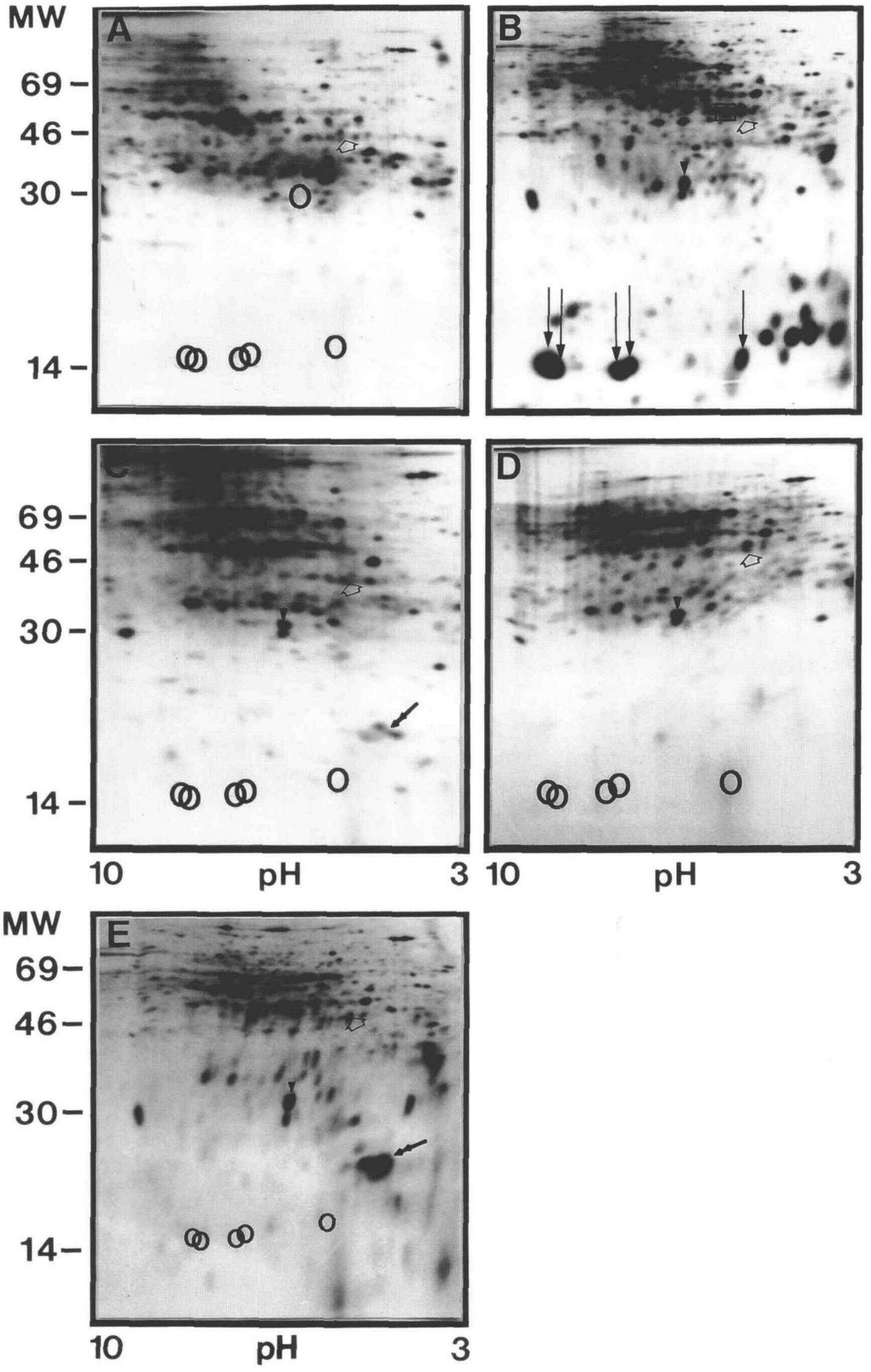
MW
A
B
69
46
30
14
C
D
69
46
30
14
10
pH
3
10
pH
3
MW
E
69
46
30
14
10
pH
3

opolysaccharide synthesis (*exo*) (Finan et al., 1985; Leigh et al., 1987) and *Agrobacterium tumefaciens* transconjugants carrying *R. meliloti* nodulation genes (Wong et al., 1983; Truchet et al., 1984; Hirsch et al., 1984, 1985) induce nodules that superficially resemble normal, nitrogen-fixing nodules. They have a central tissue surrounded by nodule parenchyma and peripheral vascular bundles, but cells of the central tissue are devoid of bacteria. Also, the nodules are not elongate like effective, nitrogen-fixing nodules but are small and broad, often with the margins of one nodule overlapping the borders of adjacent ones, like beads on a string. Meristematic activity is spread along the distal end of the nodule.

In alfalfa, two nodulins, Nms30 and MsENOD2, are associated with nodule morphogenesis. The Nms30 nodulin is known as an in vitro translation product only. Neither its amino acid sequence nor its localization in the nodule has been studied so far. The ENOD2 nodulin was originally identified as a cDNA clone from a soybean nodule library. Its deduced amino acid sequence shows a repetitive structure in which two different pentapeptides alternate, each pentapeptide starting with 2 proline residues. Because many proline-rich proteins are hydroxylated and localized in the cell wall, it is likely that ENOD2 represents a (hydroxy)proline-rich cell wall protein (Franssen et al., 1987). Recently, in situ hybridization studies have shown that the ENOD2 gene is exclusively expressed in the nodule parenchyma of soybean as well as of pea nodules (Van de Wiel et al., 1990).

Alfalfa plants can also form bacteria-free root nodule-like structures in response to the auxin transport inhibitors (ATIs) such as *N*-(1-naphthyl)phthalamic acid (NPA) and 2,3,5-triiodobenzoic acid (TIBA) (Hirsch et al., 1989). In several respects, the histology of the ATI-induced nodules resembles that of the bacteria-free ("empty") nodules elicited on alfalfa by *R. meliloti exo* mutants or *A. tumefaciens* transconjugants carrying cloned *R. meliloti nod* genes. However, their histology differs from that of bacteria-induced empty nodules in that their vascular tissue is confined to the proximal end of the nodule (Hirsch et al., 1989).

Like the *exo* mutant-induced nodules (Dickstein et al., 1988; Norris et al., 1988), the ATI-elicited nodules contain transcripts for the nodulins Nms30 and MsENOD2. Transcripts for late nodulins, such as leghemoglobin, are not found in the ATI-induced nodules (Hirsch et al., 1989). The presence of the early nodulin MsENOD2 and the nodulin Nms30 has been used as a diagnostic criterion to determine whether the ATI-induced structures were comparable with *R. meliloti*-induced root nodules. Because these nodulin genes are expressed in ATI-induced structures as well as in empty nodules formed in response to *R. meliloti exo* mutants or *A. tumefaciens* transconjugants carrying *R. meliloti* nodulation sequences, we concluded that they represent nodules fully comparable with those induced by *R. meliloti* (Hirsch et al., 1989).

In this report, we will demonstrate that the ENOD2 gene is expressed in empty nodules, both bacteria-induced and ATI-induced, in a tissue-specific manner that is the same as that of wild-type *R. meliloti*-induced nodules even though the growth pattern of the ATI-induced structures deviates from the "normal" growth pattern of alfalfa root nodules. However, even among the bacteria-induced empty nodules, there is variation in growth pattern (cf Wong et al., 1983; Hirsch et al., 1984, 1985; Finan et al., 1985). Therefore, we have included empty nodules elicited by different bacterial strains in this study. Such a comparison is significant because it demonstrates that structures that may exhibit some morphological divergence follow the same developmental pathway and are, therefore, equivalent.

RESULTS

Nodule Development and Nodulin Gene Expression

The morphology of the nodules elicited by *R. meliloti exoA* and *exoF* mutants conforms to that of other *R. meliloti exo* mutant-induced nodules, as previously described by Finan et al. (1985) and Leigh et al. (1987). Nodules induced by

Figure 1. Two-Dimensional Polyacrylamide Gel Analysis of in Vitro Translations of Total RNA Isolated from Alfalfa Tissue.

(A) From root tissue. The open arrow (in all panels) points to glutamine synthetase (see Norris et al., 1988, for identification of this translation product as GS). The circles indicate prominent translation products that are evident after in vitro translations of RNA isolated from infected root nodules but that are absent in root RNA.

(B) From nitrogen-fixing nodules induced by wild-type *R. meliloti* strain Rm1021. The boxed-in translation product is a nodule-specific/enhanced glutamine synthetase. The arrowhead points to Nms30, and the arrows indicate leghemoglobin.

(C) From Fix$^-$, bacteria-free nodules induced by Rm7055 (*exoF*::Tn*5*). Nms30 is present (arrowhead) as well as Nms25 (tandem arrows), but leghemoglobin translation products (circles) are absent.

(D) From Fix$^-$, bacteria-free nodules induced by A128 (*A. tumefaciens* carrying Rm1021 pSyma). Nms30 is present (arrowhead), but leghemoglobin translation products (circles) are not.

(E) From Fix$^-$, bacteria-free alfalfa nodules induced by Rm7061 (*exoA*::Tn*5*). The open arrow points to glutamine synthetase. The circles indicate leghemoglobin translation products observed after in vitro translation of RNA isolated from infected nodules but absent in RNA isolated from these nodules. The Nms30 translation product is present (arrowhead), as is Nms25 (tandem arrows).

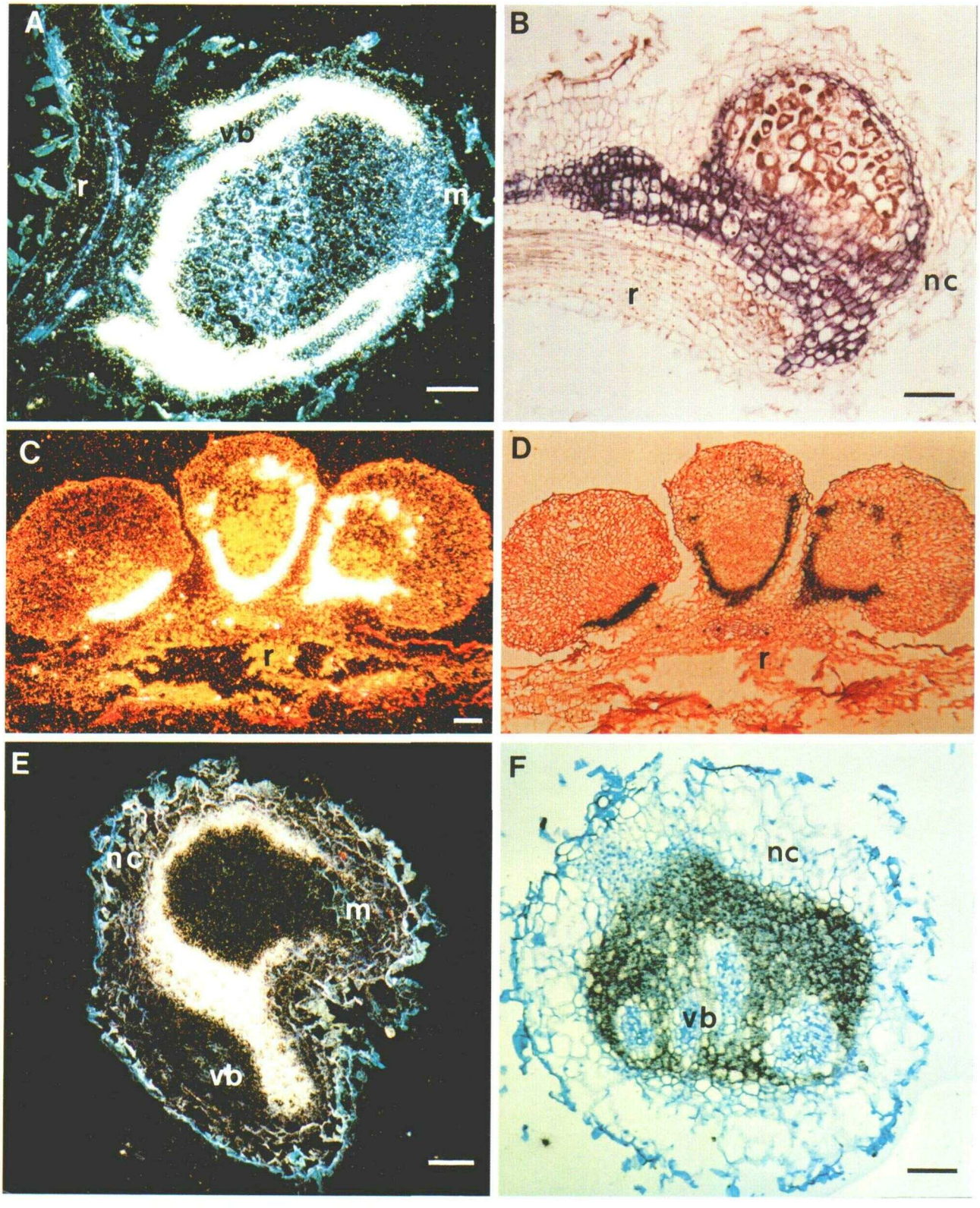

Figure 2. Detection of ENOD2 Transcript in Alfalfa Nodules by in Situ Hybridization.

A. tumefaciens strain A128, which carries the *R. meliloti* megaplasmid with the *nod* and *nif/fix* genes (pSyma), or strain A135, which contains both pSyma as well as pSymb (the megaplasmid with the *exoABDF* genes) (Finan et al., 1986) are also devoid of intracellular bacteria like the *A. tumefaciens* transconjugant-induced empty nodules reported earlier by Hirsch et al. (1984, 1985) and Truchet et al. (1984). These nodules will be described in more detail in the next section.

Previous analyses of in vitro translated RNA on two-dimensional gels have shown that about 20 different nodulin translation products can be identified in wild-type *R. meliloti*-induced alfalfa nodules, as seen in Figures 1A and 1B. In nodules formed in response to *R. meliloti exo* mutants or *A. tumefaciens* transconjugants carrying *R. meliloti* nodulation genes, only the nodulin translation product Nms30 can be detected (Dickstein et al., 1988; Norris et al., 1988). In addition, a nodulin of variable isoforms, Nms25, that appears to be unique to *exo* mutant-induced nodules, has been described by Leigh et al. (1987). Figures 1C and 1E illustrate that the empty nodules used in the present study conformed to this pattern of gene expression. Nms30 as well as Nms25 translation products were detectable in nodules elicited by *exoF* and *exoA* mutants. On the other hand, nodules formed in response to A128 inoculation appeared to contain only the Nms30 transcript (Figure 1D).

The early nodulin ENOD2 mRNA has been shown by RNA transfer blot analysis to be present in *exo* mutant-induced nodules as well as in *A. tumefaciens* transconjugant-elicited nodules (Dickstein et al., 1988). A similarly sized 1.4-kb ENOD2 transcript was detected in nodules induced by the *A. tumefaciens* transconjugants A128 and A135 used in the present study (data not shown).

Thus, the pattern of nodulin gene expression is remarkably similar in all empty nodules, except that the nodulin Nms25 transcript apparently occurs only in *R. meliloti exo* mutant-induced nodules.

Localization of ENOD2 Transcripts in Nodules

Sections of the various alfalfa root nodules were hybridized to antisense RNA transcribed from pA2ENOD2, which contains an approximately 0.3-kb insert of alfalfa ENOD2 cDNA. The 4-week-old, wild-type *R. meliloti*-induced nodule showed a hybridization pattern like the one described for pea (cf Van de Wiel et al., 1990). The ENOD2 mRNA was present in parenchyma cells (nodule parenchyma) surrounding the central tissue of infected and uninfected cells and also at the base of the nodule, as shown in Figures 2A and 2B. There was no ENOD2 transcript detectable at the top of the nodule, the site of the apical meristem (Figure 2A). Three-dimensionally, ENOD2 localization was in the shape of a cup, which was open at the nodule meristem. No ENOD2 transcripts were found within the vascular strands along the periphery of the nodule (Figure 2A).

Two-week-old to 3-week-old NPA-induced and TIBA-induced nodules were more or less similar to each other (data not shown). Meristematic activity was frequently spread over a relatively large part of the distal end of the nodule instead of being concentrated to the apex, as in wild-type *R. meliloti*-induced nodules. Vascular traces were confined to the proximal part of the nodule and did not separate into distinct strands extending distally into the peripheral tissue of the nodule. A peripheral tissue and central tissue, the latter consisting of cells rich in plastids with prominent starch grains, can be distinguished (Figure 2C). Around this central tissue, a relatively narrow zone consisting of highly vacuolated, densely packed cells contained transcripts that hybridized to the ENOD2 antisense

Figure 2. (continued).

(A) Dark-field photograph of a nitrogen-fixing alfalfa nodule. ENOD2 transcripts as visualized by the brightly reflecting silver grains (see Methods) are localized to parenchyma cells along the periphery of the nodule surrounding the vascular bundle (vb) and also along the base of the nodule. The meristem (m) is devoid of MsENOD2 transcript. Median longitudinal section. Magnification ×85. Bar = 100 μm.

(B) Bright-field photograph of a nitrogen-fixing nodule cut obliquely. The nodule meristem is out of the plane of section. ENOD2 transcripts were localized on paraffin sections using the Boehringer Mannheim RNA labeling kit (Genius) (see Methods). A blue color is present in parenchyma cells along the edge of the infected cells and at the base of the nodule but not in the nodule cortex (nc). The color that appears to be in the root (r) is actually at the base of a second lobe of a two-lobed nodule. The second lobe is not observed in this section. Magnification ×85. Bar = 100 μm.

(C) Dark-field photograph of a cluster of nodules elicited 2 weeks after addition of NPA. ENOD2 transcripts (brightly reflecting silver grains) are detected along the periphery of the nodule, but not in the root (r). Slightly oblique section. Magnification ×40. Bar = 100 μm.

(D) Bright-field photograph of **(C)**. Magnification ×40.

(E) Dark-field photograph of a 5-week-old, bacteria-free nodule elicited by Rm5078 (*exoB*::Tn*5*). The nodule meristem (m) is devoid of ENOD2 mRNA, as is the nodule cortex (nc). ENOD2 transcripts extend along the periphery of the nodule and are also localized to parenchyma cells at the base of the nodule. The vascular bundle (vb; observed in transverse section) is also devoid of ENOD2 transcript. Nonmedian longitudinal section. Magnification ×85. Bar = 100 μm.

(F) Bright-field photograph of a bacteria-free nodule induced by Rm7061 (*exoA*::Tn*5*). The nodule has been sectioned transversely (see Figure 3A for approximate location of the section). Several vascular bundles (vb) are evident; these are surrounded by parenchyma cells that express MsENOD2. The nodule cortex (nc) is devoid of ENOD2 mRNA. Magnification ×85. Bar ≈ 100 μm.

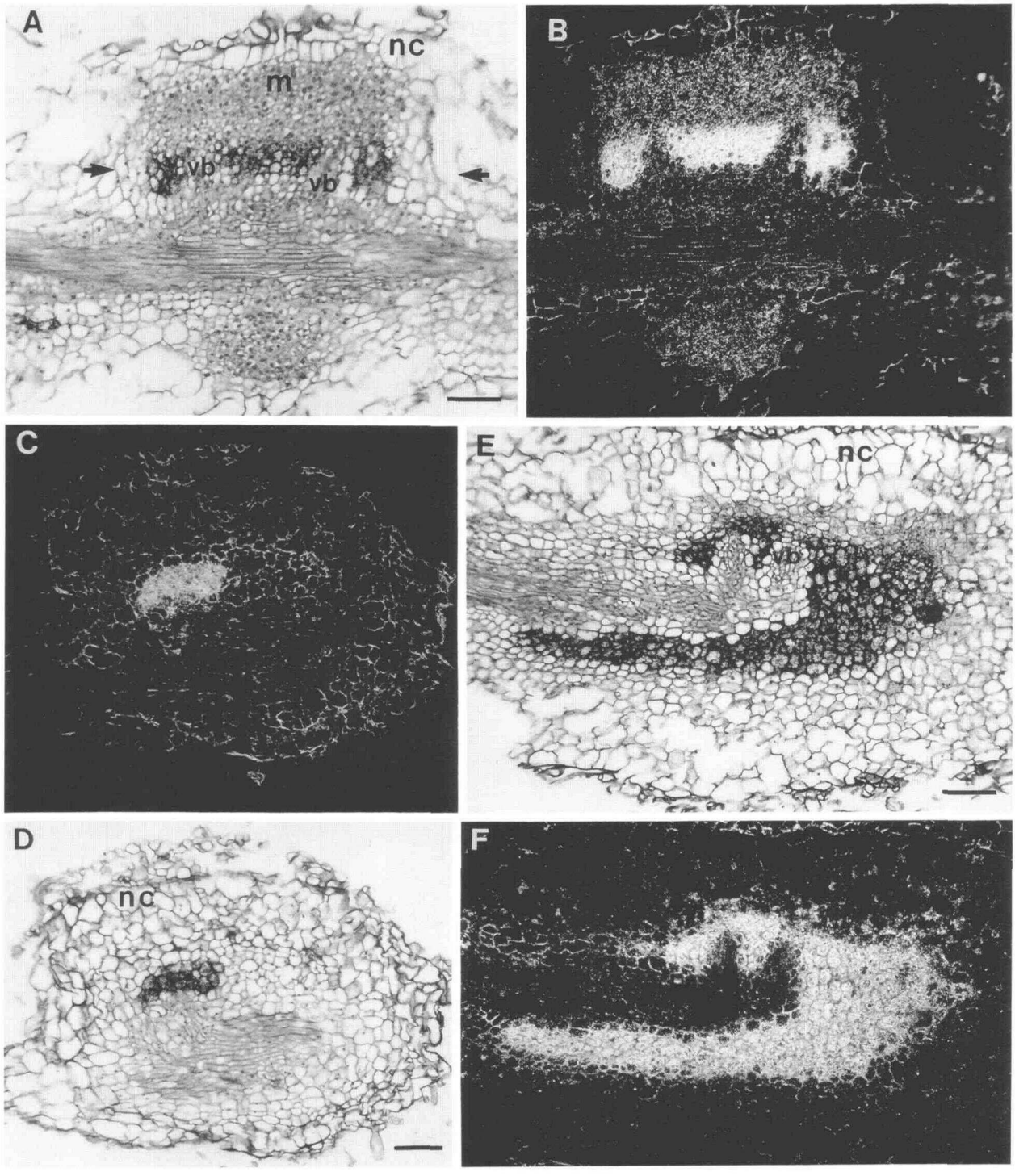

Figure 3. Detection of ENOD2 Transcript in Alfalfa Nodules by in Situ Hybridization.

(A) Bright-field photograph of a 3-week-old, bacteria-free nodule induced by Rm5078 (*exoB*::Tn*5*). The presumed meristematic region (m) is very broad and lacks ENOD2 mRNA. ENOD2 transcripts are detected at the base of the nodule in parenchyma tissue that surrounds

RNA (Figures 2C and 2D). Outside this zone, a less densely packed nodule cortex, where no ENOD2 transcript could be detected, was present.

Figure 2E illustrates an example of a 5-week-old *exoB* mutant-induced nodule. As in wild-type *R. meliloti*-induced nodules, it is possible to distinguish an apical meristem, a nodule cortex, a peripheral zone, and a central tissue, which, however, was free of intracellular bacteria. ENOD2 transcript was found in the densely packed, highly vacuolated parenchymatous tissue that constitutes the inner part of the peripheral tissue. This parenchymatous tissue was traversed by a vascular strand that is free of ENOD2 transcript (data not shown). The outer part of the peripheral tissue, which is more loosely packed, was also free of ENOD2 transcript.

The majority of *exoB*, *exoA*, or *exoF* mutant-induced nodules are not elongate like effective, nitrogen-fixing alfalfa nodules. They are small and broad, often with the margins of one nodule overlapping the borders of adjacent ones, thus giving the appearance of beads on a string. Meristematic activity, which is spread along a relatively long region of the subtending root, leads to the deposition of a limited amount of tissue in a plane perpendicular to the root axis. Consequently, little peripheral and central tissue is formed at the apical end of the nodule, as shown in Figures 3A and 3B. ENOD2 transcripts were localized to nodule parenchyma cells at the base of the nodule. Also at the base of the nodule, several vascular traces connected to the root stele were present that did not contain ENOD2 transcript (Figures 2F, 3A, and 3B). A more distally located tissue consisting of cytoplasmically rich cells containing amyloplasts was also free of ENOD2 transcript (Figures 3A and 3B).

The nodules elicited by the *A. tumefaciens* transconjugants A128 and A135 were quite similar to the small, beadlike, *exo* mutant-induced nodules described above. There was a limited amount of meristematic activity over a broad zone of the subtending root (Figures 3C to 3F). Proximally, several vascular traces were connected to the root stele (Figures 3E and 3F). ENOD2 transcripts were clearly detectable in a zone of densely packed, vacuolated parenchymatous tissue, containing amyloplasts, at the base of these nodules and around the vascular traces. The distal tissue of these nodules, which is highly vacuolated and free of amyloplasts, contained no ENOD2 transcript (Figure 3D).

DISCUSSION

Our in situ hybridization studies clearly showed that the ENOD2 gene was expressed in the nodule parenchyma of nitrogen-fixing alfalfa nodules, following a pattern in agreement with the recent observations of pea nodules (Van de Wiel et al., 1990). Moreover, we found that the ENOD2 gene was expressed in a tissue-specific manner in nodules elicited by the ATIs, NPA, and TIBA: ENOD2 transcripts were present in a zone of densely packed, highly vacuolated parenchyma cells between a central tissue of cells, rich in amyloplasts, and an outer layer of more loosely packed cortical tissue. No ENOD2 mRNA was detected in the distal end of the nodule. The position and morphology of the ENOD2 gene-expressing zone corresponded to those of the nodule parenchyma of wild-type *R. meliloti*-induced nodules. Hence, by using the criterion of tissue-specific ENOD2 gene expression, one may conclude that the empty ATI-elicited nodules are indeed comparable with nodules induced by wild-type *R. meliloti*.

The *R. meliloti exo* mutants and *A. tumefaciens* transconjugants induce a heterogeneous population of nodules (cf Wong et al., 1983; Hirsch et al., 1984, 1985; Finan et al., 1985). Relatively few are of the elongate type that most resemble wild-type *R. meliloti*-induced nodules. In such nodules, the presence of ENOD2 transcripts was restricted to a tissue that, both positionally and morphologically, was comparable with the nodule parenchyma of wild-type *R. meliloti*-induced nodules (cf Figure 2E and Figures 2A and 2B). The vast majority of nodules, however, were small and broad, in which little peripheral and central tissue was differentiated perpendicularly to the long axis of the root. Nevertheless, ENOD2 gene expression was restricted to a zone of densely packed parenchymatous tissue extending along the base of the nodule and around the vascular traces (Figures 3A and 3B). The location of this zone was the same as the ENOD2 gene-expressing

Figure 3. (continued).

the vascular bundles (vb). The nodule cortex (nc) forms the outer boundary of the nodule. The arrows denote the approximate location of the transverse section illustrated in Figure 2F. Near median longitudinal section. Magnification ×82.5. Bar = 100 μm.

(B) Dark-field photograph of **(A)**. Magnification ×82.5.

(C) Dark-field photograph of a bacteria-free nodule induced by A135. ENOD2 transcripts are localized to the parenchyma cells at the base of the nodule. Oblique section. Magnification ×82.5.

(D) Bright-field photograph of **(C)**. ENOD2 mRNA is localized to the base of the nodule. A nodule cortex (nc) is observed, but cells typical of a meristematic region are not identifiable in this nodule. Magnification ×82.5. Bar = 100 μm.

(E) Bright-field photograph of a bacteria-free nodule formed in response to A128 infection. The nodule is sectioned transversely to obliquely. ENOD2 mRNA is detected at the base of the nodule surrounding the vascular bundles (vb). Isodiametric, dividing cells typical of a meristematic region are not observed in this nodule, but the loosely packed nodule cortex (nc) is present. Magnification ×82.5. Bar = 100 μm.

(F) Dark-field photograph of **(D)**.

nodule parenchyma region in wild-type *R. meliloti*-induced nodules. Thus, in spite of the morphological anomalies caused by the diffuse and limited meristematic activity in these empty nodules, the pattern of ENOD2 expression did not differ fundamentally from that observed in wild-type *R. meliloti*-induced nodules.

Localization studies of mRNAs that mark specific nodule tissues may provide insight into the nature of aberrant root nodules. Although distinct tissues, like nodule parenchyma, should be recognizable by the combination of positional and morphological criteria, such distinctions in tissue types are relatively difficult to assess by microscopical studies alone, especially in small and broad empty nodules of the type described above. In the cases where a clearly differentiated nodule endodermis is detectable (cf Truchet et al., 1984; Finan et al., 1985), it is relatively easy to delimit nodule parenchyma cells from the more loosely packed ("outer") cortex. However, delimitation from a bacteria-free central tissue is frequently more difficult because possible differences in the extent of intercellular space between the two tissues are not easy to discern. Furthermore, other morphological criteria are difficult to evaluate; the nodule parenchyma cells are often rich in amyloplasts, like the central tissue itself. Also, the extent of vacuolation in the central tissue is variable in nodules of the small and broad type. In these cases, localization studies of ENOD2 transcripts are helpful. Such analysis may also be important for understanding even more peculiar types of nodules, such as those elicited on clover by *A. tumefaciens* or *R. leguminosarum* bv *trifolii* transconjugants carrying *R. meliloti* nodulation sequences (Hirsch et al., 1985; Truchet et al., 1985), or the ones elicited on alfalfa by *R. meliloti* with a Tn5 insertion 3 kb downstream from *nodC* (Dudley et al., 1987). Unlike other empty nodules, these pseudonodules more closely resemble lateral roots in that they have a centrally located vascular bundle. In contrast to normal lateral roots, however, one such type of nodule has a nodule endodermis-like layer in its cortex (Dudley et al., 1987). Localization of ENOD2 transcripts may indicate whether a nodule parenchyma-like tissue is present in these pseudonodules and, if so, where it is located. It may further indicate whether these structures are developmentally equivalent to authentic root nodules.

Thus, based on the observation that the ATIs induce a normal pattern of ENOD2 gene expression, we conclude that in their action the ATIs mimic some factor(s) responsible for nodule development. The ATIs are known to cause alterations in the endogenous hormone balance of the plant. Cell divisions and ENOD2 gene expression, both of which are induced by ATI treatment, thus may be related to the hormonal status of the root. Recently, Lerouge et al. (1990) have identified a *Rhizobium*-produced molecule, NodRm-1, which elicits alfalfa root hair deformation, as a β-sulfated tetraglucosamine with acetyl and acyl substitutions. The ATIs, which are often substituted benzoic acids, are structurally different from NodRm-1, an oligosaccharide. Thus, it is unlikely that both act at the same site. This implies that *Rhizobium* may produce other molecules, separate from NodRm-1, that trigger the cascade of events leading to nodule development. Alternatively, NodRm-1 may stimulate the production of an endogenous plant factor that interacts with the same site as the ATIs.

METHODS

Plant Material

Alfalfa (*Medicago sativa* L cv Iroquois) plants were grown as described by Norris et al. (1988). At the time of sowing, individual bins containing alfalfa seeds were left uninoculated or inoculated with either *Rhizobium meliloti* wild-type strains Rm2011 or Rm1021, *R. meliloti* mutant in *exoB* (Rm5078), *exoA* (Rm7061), or *exoF* (Rm7055), or *Agrobacterium tumefaciens* transconjugants, either strain A128, which harbors the *nod/nif* symbiotic megaplasmid (pSyma), or strain A135, which carries the *nod/nif* megaplasmid (pSyma) and the megaplasmid bearing *exo* genes (pSymb) (Leigh et al., 1985; Finan et al., 1986). Plants were treated with the ATIs as described previously (Hirsch et al., 1989).

RNA Analysis

Tissue was harvested, frozen in liquid nitrogen, and stored at −80°C until use. Total RNA was isolated from nodule or root tissue, in vitro translations were performed, and the translation products were separated by two-dimensional electrophoresis as described by Norris et al. (1988). The RNA for transfer blots was transferred to GeneScreen (Du Pont-New England Nuclear) according to the manufacturer's directions. A 292-bp insert of pA2ENOD2 (Dickstein et al., 1988) was prepared and nick translated. Hybridization and washing conditions followed the GeneScreen manufacturer's protocol, washing at 65°C.

In Situ Hybridization

Tissues were fixed either as described by Van de Wiel et al. (1990) or in 4% glutaraldehyde, 1.5% paraformaldehyde in 0.1 M phosphate buffer, pH 7.2. After fixation, the tissues were rinsed twice in buffer and dehydrated in a graded alcohol series until they were in 50% alcohol. The tissues were then transferred to the first tertiary butyl alcohol step, dehydrated in the tertiary butyl alcohol series (Sass, 1958), and embedded in Paraplast. Sections either 7 μm or 8 μm thick were affixed to poly-L-lysine-coated slides. The in situ hybridizations using ^{35}S-UTP antisense RNA probes were based on a protocol published by Cox and Goldberg (1988) and were performed essentially as described by Van de Wiel et al. (1990). After development of the emulsion, sections were stained either with 1% aqueous safranin or with 0.05% toluidine blue.

Alternatively, the RNA labeling kit (Genius) using digoxigenin-labeled UTP (Boehringer Mannheim) was utilized. Sense and antisense probes were made according to the manufacturer's directions and added to deparaffinized sections that had been

pretreated as described for radioactive probes. Some nodules were fixed overnight in formaldehyde-acetic acid-alcohol (Sass, 1953), rinsed overnight in 50% alcohol, slowly rehydrated, and then frozen on a block in liquid nitrogen. The nodules were sectioned at 16 μm using a cryostat, and the sections were placed on poly-L-lysine-coated slides. The nodule sections were gradually warmed to room temperature and further treated as for radioactive probes. Antisense probe was added to the cryostat-sectioned material at 10 ng/mL to 100 ng/mL of hybridization buffer per slide. The manufacturer's protocol for pre-hybridization, hybridization, and post-hybridization was followed for both sense and antisense probes; sections were hybridized at 37°C overnight. MsENOD2 transcripts were detected immunologically according to the manufacturer's directions. For paraffin-embedded material, 12 hr to 72 hr were required for maximal color development, whereas for cryostat-sectioned material, color development generally occurred within 60 min. The sections were not counterstained.

After dehydration through an alcohol series, the sections were mounted with DPX or Eukitt, and were photographed either with a Nikon or Zeiss Axiophot microscope equipped with bright-field and dark-field optics.

ACKNOWLEDGMENTS

We acknowledge the generosity of Agway, Inc., Syracuse, NY, for providing us with alfalfa seeds, and we also thank Ethan R. Signer, John Leigh, and Turlough Finan for bacterial strains. We are especially grateful to Judith Lengyel, who introduced us to the "Genius Kit," and to Stefan Kirchanski for critically reading the manuscript. We also thank the members of our respective laboratories for helpful comments and useful discussions. A.M.H. was supported at the beginning of this project by a fellowship from the Organization for Economic Cooperation and Development on Food Production and Preservation (summer 1988). We also acknowledge support from National Science Foundation Grant DCB-8703297.

Received June 20, 1990; accepted August 13, 1990.

REFERENCES

Cox, K.H., and Goldberg, R.B. (1988). Analysis of plant gene expression. In Plant Molecular Biology: A Practical Approach, C.H. Shaw, ed (Oxford: IRL Press), pp. 1–34.

Dickstein, R., Bisseling, T., Reinhold, V.N., and Ausubel, F.M. (1988). Expression of nodule-specific genes in alfalfa root nodules blocked at an early stage of development. Genes Dev. **2,** 677–687.

Dudley, M.E., Jacobs, T.W., and Long, S.R. (1987). Microscopic studies of cell divisions induced in alfalfa roots by *Rhizobium meliloti*. Planta **171,** 289–301.

Finan, T.M., Hirsch, A.M., Leigh, J.A., Johansen, E., Kuldau, G.A., Deegan, S., Walker, G.C., and Signer, E.R. (1985). Symbiotic mutants of *Rhizobium meliloti* that uncouple plant from bacterial differentiation. Cell **40,** 869–877.

Finan, T.M., Kunkel, B., De Vos, G.F., and Signer, E.R. (1986). Second symbiotic megaplasmid in *Rhizobium meliloti* carrying exopolysaccharide and thiamine synthesis genes. J. Bacteriol. **167,** 66–72.

Franssen, H.J., Nap, J.P., Gloudemans, T., Stikema, W., Van Dam, H., Govers, F., Louwerse, J., Van Kammen, A., and Bisseling, T. (1987). Characterization of cDNA for nodulin-75 of soybean: A gene product involved in early stages of root nodule development. Proc. Natl. Acad. Sci. USA **84,** 4495–4499.

Hirsch, A.M., Wilson, K.J., Jones, J.D.G., Bang, M., Walker, V.V., and Ausubel, F.M. (1984). *Rhizobium meliloti* nodulation genes allow *Agrobacterium tumefaciens* and *Escherichia coli* to form pseudonodules on alfalfa. J. Bacteriol. **158,** 1133–1143.

Hirsch, A.M., Drake, D., Jacobs, T.W., and Long, S.R. (1985). Nodules are induced on alfalfa roots by *Agrobacterium tumefaciens* and *Rhizobium trifolii* containing small segments of the *Rhizobium meliloti* nodulation region. J. Bacteriol. **161,** 223–230.

Hirsch, A.M., Bhuvaneswari, T.V., Torrey, J.G., and Bisseling, T. (1989). Early nodulin genes are induced in alfalfa root outgrowths elicited by auxin transport inhibitors. Proc. Natl. Acad. Sci. USA **86,** 1244–1248.

Leigh, J.A., Signer, E.R., and Walker, G.C. (1985). Exopolysaccharide-deficient mutants of *Rhizobium meliloti* that form ineffective nodules. Proc. Natl. Acad. Sci. USA **82,** 6231–6235.

Leigh, J.A., Reed, J.W., Hanks, J.F., Hirsch, A.M., and Walker, G.C. (1987). *Rhizobium meliloti* mutants that fail to succinylate their calcofluor-binding exopolysaccharide are defective in nodule invasion. Cell **51,** 579–587.

Lerouge, P., Roche, P., Faucher, C., Maillet, F., Truchet, G., Promé, J.C., and Dénarié, J. (1990). Symbiotic host-specificity of *Rhizobium meliloti* is determined by a sulphated and acylated glucosamine oligosaccharide signal. Nature **344,** 781–784.

Norris, J.H., Macol, L.A., and Hirsch, A.M. (1988). Nodulin gene expression in effective alfalfa nodules and in nodules arrested at three different stages of development. Plant Physiol. **88,** 321–328.

Sass, J.E. (1953). Botanical Microtechnique, 3rd ed (Ames, IA: Iowa State University Press), pp. 26–28.

Truchet, G., Rosenberg, C., Vasse, J., Julliot, J.-S., Camut, S., and Dénarié, J. (1984). Transfer of *Rhizobium meliloti* Sym genes into *Agrobacterium tumefaciens*: Host-specific nodulation by atypical infection. J. Bacteriol. **157,** 134–142.

Truchet, G., Debelle, F., Vasse, J., Terzaghi, B., Garnerone, A.-M., Rosenberg, C., Batut, J., Maillet, F., and Dénarié, J. (1985). Identification of a *Rhizobium meliloti* pSym2011 region controlling the host specificity of root hair curling and nodulation. J. Bacteriol. **164,** 1200–1210.

Van de Wiel, C., Scheres, B., Franssen, H., van Lierop, M.-J., Van Lammeren, A., Van Kammen, A., and Bisseling, T. (1990). The early nodulin transcript ENOD2 is located in the nodule parenchyma (inner cortex) of pea and soybean root nodules. EMBO J. **9,** 1–7.

Witty, J.F., Minchin, F.R., Skøt, L., and Sheehy, J.E. (1986). Nitrogen fixation and oxygen in legume root nodules. Oxford Surv. Plant Mol. Cell Biol. ,**3,** 275–314.

Wong, C.H., Pankhurst, C.E., Kondorosi, A., and Broughton, W.J. (1983). Morphology of root nodules and nodule-like structures formed by *Rhizobium* and *Agrobacterium* strains containing a *Rhizobium meliloti* megaplasmid. J. Cell Biol. **97,** 787–794.